CHAPTER IV
RESULTS AND DISCUSSION

4.1 Effects of Feed Composition on the *m*- and *p*-CNB Crystallization

The purpose of this part is to study the effects of feed compositions on the *m*- and *p*-CNB crystallization and to construct the binary phase diagram. The feed solution was seven grams of *m*- and *p*-CNB with different *m*-CNB compositions (20.0, 30.0, 40.0, 61.0, 62.9, 65.0, 70.0, 80.0 and 90.0 wt% *m*-CNB). Tables 4.1 and 4.2 show the crystallization temperature and the feed and precipitate compositions from two separate experiments. It can be clearly seen that the experiment is reproducible.

Table 4.1 Composition of *m*- and *p*-CNB in the feeds and crystals, and crystallization temperatures run#1

Feed	Feed composition (wt%)		Precipitate composition (wt%)		Crystallization temperature (°C)
	m-CNB	*p*-CNB	*m*-CNB	*p*-CNB	
Below the eutectic	20.10	79.90	3.48	96.52	68.0
	29.86	70.14	3.59	96.41	57.0
	39.88	60.12	4.80	95.20	48.0
	61.01	38.99	4.98	95.02	24.0
The eutectic	62.90	37.10	62.89	37.11	23.0
Above the eutectic	65.05	34.95	93.53	6.47	24.0
	70.02	29.98	96.56	3.44	25.0
	80.17	19.83	97.70	2.30	28.5
	90.32	9.68	98.64	1.36	34.0

Table 4.2 Composition of *m*- and *p*-CNB in the feeds and crystals, and crystallization temperatures run#2

Feed	Feed composition (wt%)		Precipitate composition (wt%)		Crystallization temperature (°C)
	m-CNB	*p*-CNB	*m*-CNB	*p*-CNB	
Below the eutectic	20.03	79.97	2.20	97.80	68.0
	30.02	69.98	3.26	96.74	57.0
	40.07	59.93	5.56	94.44	48.0
	61.05	38.95	5.85	94.15	24.0
The eutectic	62.89	37.11	62.91	37.09	23.0
Above the eutectic	65.03	34.97	94.58	5.42	24.0
	70.07	29.93	97.70	2.30	25.0
	80.00	20.00	98.70	1.30	28.5
	90.02	9.98	97.94	2.06	34.0

The starting feed composition and the precipitate composition with different *m*-CNB are shown in Tables 4.1 and 4.2. The crystallization of the feed below the eutectic composition (20, 30, 40, 61 wt% *m*-CNB) results in the crystal form. The composition is rich in *p*-CNB. On the contrary, where the feed composition at the eutectic composition (62.9 wt% *m*-CNB) is cooled down to the crystallization temperature at 23.0 °C, an amorphous solid with the composition close to the feed composition can be observed. Crystallization of the feed above the eutectic composition results in the crystal form, which is the same with that below the eutectic composition but the composition is rich in *m*-CNB. As a whole, the result shows the purity of the precipitate composition is not close to 100 wt%. In the industrial crystallization practice, many bulk-produced chemicals with a purity more than 95 percent are often accepted as justifying the designation "pure". Generally, crystals contain foreign impurities or called "inclusion". It tends to trap mother liquor or impurity inside a crystal that have not been removed by washing. It is a reason why a single crystallization step cannot produce 100 percent (Mullin, 2001).

The binary phase diagram of *m*- and *p*-CNB was constructed between the feed composition of *m*-CNB and crystallization temperature, as shown in Figure 4.1. The thermodynamic equilibrium of the equilibrium binary phase diagram of *m*- and *p*-CNB can be explained by phase rule. Phase rule helps to characterize state of the system, predicts the equilibrium relations of phase, and helps to construct the phase diagram. The phase rule describes the possible number of degrees of freedom in a chemical system at equilibrium. The number of variables are the number of chemical components in the system, temperature, and pressure. The number of phases present depend on the variance or degrees of freedom of the system. It was deduced from the thermodynamic principles by J. W. Gibbs in the 1870s. The general form of the phase rule is stated as follows (Mullin, 2001):

$$P + F = C + 2 \tag{4.1}$$

where F is the number of degrees of freedom or variance of the system,

- F = 0 invariant (no change in system),
- F = 1 univariant (equilibrium line),
- F = 2 divariant (stable phase region),
- F < 0 then there must be disequilibrium,

C is the number of components, as defined above, in the system,

P is the number of phases in equilibrium.

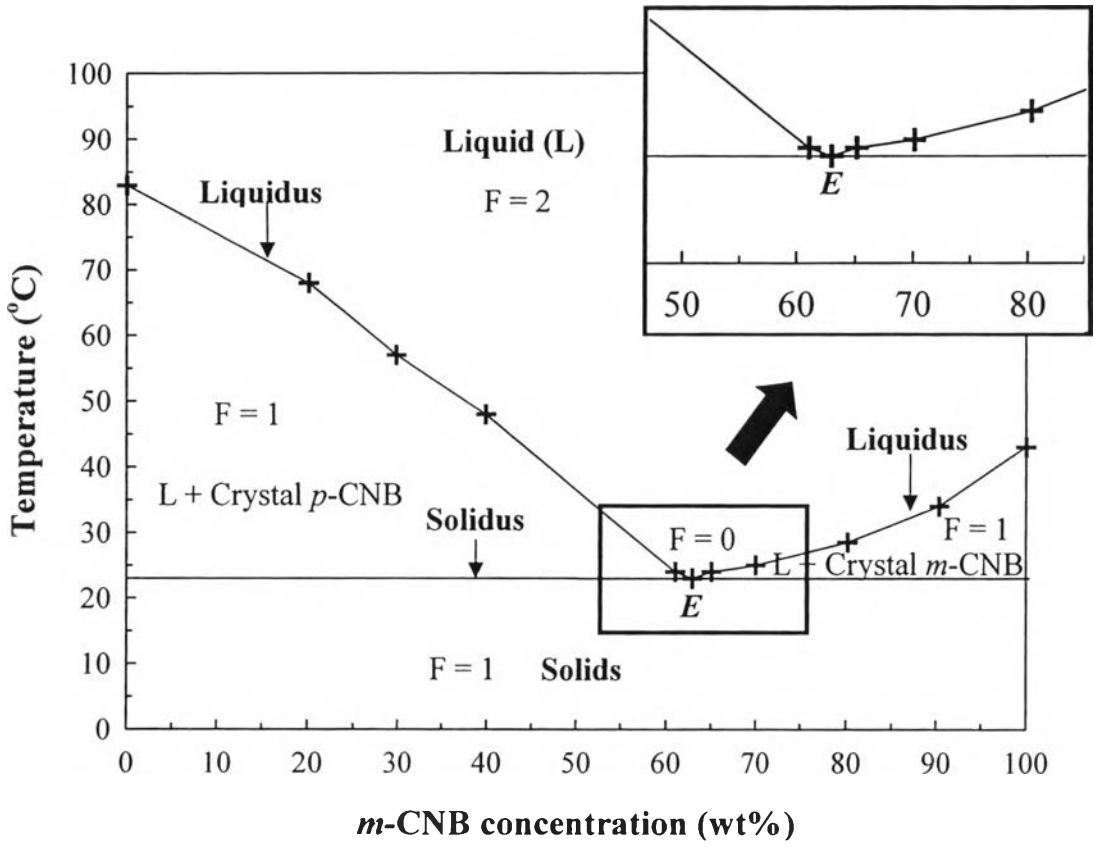

Figure 4.1 Degree of freedom of the binary phase diagram of *m*- and *p*-CNB.

The binary phase diagram of *m*- and *p*-CNB is plotted between temperature (axis X) and composition (axis Y) at the constant pressure (1 atm).

From the phase rule: $F = C - P + 1$

Above the liquidus line: liquid *m*-CNB + *p*-CNB

$$F = C - P + 1$$

$$F = 2 - 1 + 1$$

$$F = 2$$

For F = 2 (divariant), this is stable on the phase diagram. Both temperature and pressure can change without affecting the number of phase present.

The area between under the liquidus line to solidus line: liquid *m*-CNB + *p*-CNB and solid *m*-CNB or liquid *m*-CNB + *p*-CNB and solid *p*-CNB

$$F = C - P + 1$$

$$F = 2 - 2 + 1$$

$$F = 1$$

For F = 1 (univariant), there is only one independent variable that can be changed without affecting the number of phases.

At the eutectic temperature: solid *m*-CNB, solid *p*-CNB and liquid *m*-CNB + *p*-CNB

$$F = C - P + 1$$

$$F = 2 - 3 + 1$$

$$F = 0$$

F = 0 (invariant), a one component system has no degree of freedom when three phases are in equilibrium.

Under the solidus line: solid *m*-CNB and solid *p*-CNB

$$F = C - P + 1$$

$$F = 2 - 2 + 1$$

$$F = 1$$

The binary phase diagram of *m*- and *p*-CNB can be further explained from Figure 4.2.

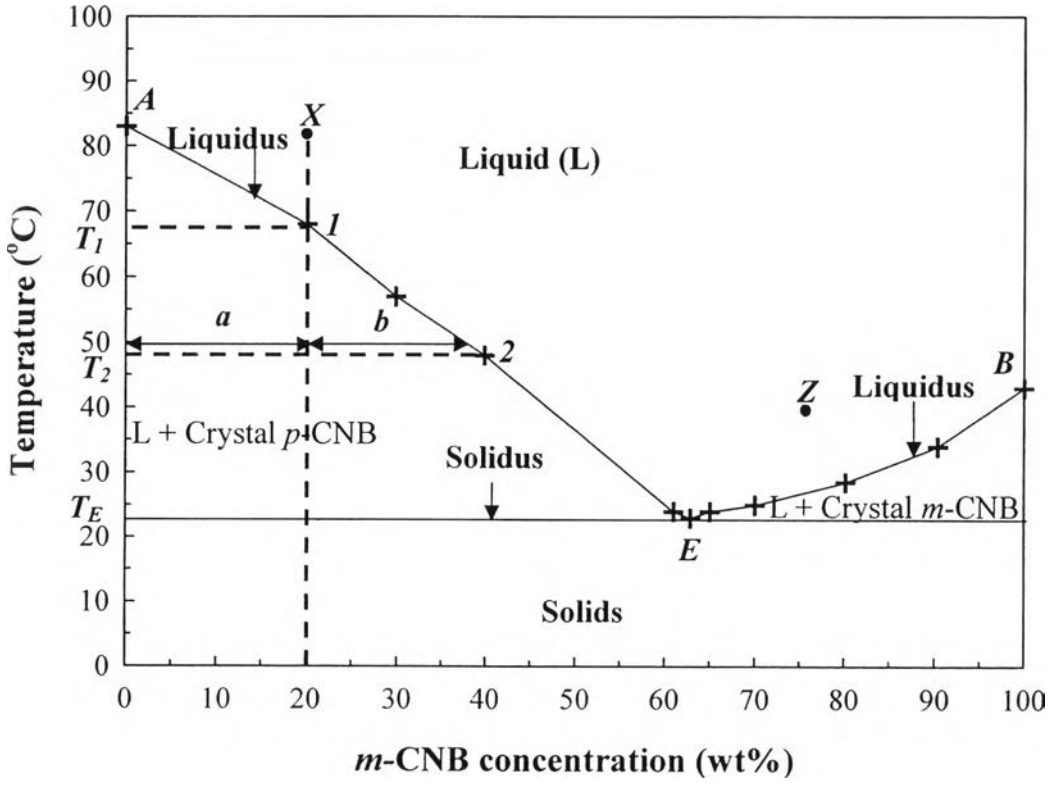

Figure 4.2 Binary phase diagram of *m*- and *p*-CNB.

The binary phase diagram of *m*- and *p*-CNB from Figure 4.2 shows the crystallization temperature in each feed composition and phase of solutions. Melting or freezing point of *p*-CNB is 83.5 °C represented by point ***A*** and melting point of *m*-CNB is 44.5 °C, point ***B***. Homogeneous liquid phases of *m*- and *p*-CNB represent above the liquidus line. Point ***X*** consists of two liquid components, *m*- and *p*-CNB (20 wt% *m*-CNB, 80 wt% *p*-CNB). When the solution (***X***) is cooled to the liquidus line, the first crystal solid of *p*-CNB begins to form. The liquid component has lower *p*-CNB concentration and higher *m*-CNB concentration. If the solution is further cooled to T_2, there will be crystal solid of *p*-CNB and solution of *m*- and *p*-CNB. The composition of the system remains unchanged. The percent weight of liquid and solid phases of the binary equilibrium phase diagram can be determined by the lever rule.

$$\text{Percent weight of } p\text{-CNB} = \frac{b}{a+b} \tag{4.2}$$

$$\text{Percent weight of liquid} = \frac{a}{a+b} \tag{4.3}$$

If the solution is cooled down to below the solidus line, the solution becomes solid. If the solution at point ***Z*** is cooled down, similar results from cooling down the solution at point ***X*** can be observed but the *m*-CNB crystal solid forms. From the binary phase diagram, the eutectic composition is point ***E***. The eutectic is a physical mixture, not a chemical compound. The eutectic composition is the mixture of two or more phases at composition that has the lowest melting point, and where the phases simultaneously crystallize from molten solution at this temperature. The eutectic composition in this phase diagram is 62.9 wt% *m*-CNB and 37.1 wt% *p*-CNB with the crystallization temperature at 23.0 °C. At this point, a completely solidified mixture of *m*-CNB and *p*-CNB is formed. Below the eutectic temperature or solidus line, all of mixtures are solid (Mullin, 2001).

4.2 Effects of KY Zeolite on the Crystallization and Composition of *m*- and *p*-CNB

4.2.1 Effects of KY Zeolite on the CNB Feed Solution Compositions

A phase diagram study with the presence of KY zeolite on the crystallization was studied by using the feed solution of seven grams of *m*- and *p*-CNB with different *m*-CNB compositions below the eutectic, at the eutectic, and above the eutectic composition. Effect of adding the KY zeolite on the feed composition from two separate experiments are shown in Tables 4.3-4.4.

Table 4.3 *m*- and *p*-CNB composition in the feed with different wt% of *m*-CNB before and after adding 5 grains of KY zeolite run#1

Feed	Feed composition before adding KY zeolite (wt%)		Precipitate composition after adding KY zeolite (wt%)		% difference*
	m-CNB	*p*-CNB	*m*-CNB	*p*-CNB	
Below the eutectic	20.01	79.99	20.03	79.97	+0.02
	30.03	69.97	30.01	69.99	-0.02
	40.02	59.98	40.05	59.95	+0.03
	61.03	38.97	61.01	38.99	-0.02
The eutectic	62.93	37.07	62.92	37.08	-0.01
Above the eutectic	65.02	34.98	65.00	35.00	-0.02
	70.00	30.00	70.05	29.95	+0.05
	80.04	19.98	79.99	20.01	+0.05
	90.01	9.99	90.03	9.97	+0.02

* %difference is the difference between the *m*-CNB composition in the feed with and without adsorbent.

Table 4.4 *m*- and *p*-CNB composition in the feed with different wt% of *m*-CNB before and after adding 5 grains of KY zeolite run#2

Feed	Feed composition before adding KY zeolite (wt%)		Precipitate composition after adding KY zeolite (wt%)		% difference*
	m-CNB	*p*-CNB	*m*-CNB	*p*-CNB	
Below the eutectic	20.04	79.96	20.03	79.97	-0.01
	29.97	70.03	29.94	70.06	-0.03
	40.01	59.99	39.97	60.03	-0.04
	61.06	38.98	61.02	38.99	-0.04
The eutectic	62.95	37.09	62.90	37.10	-0.05
Above the eutectic	65.03	34.97	65.00	35.00	-0.03
	69.96	30.04	70.01	29.95	+0.05
	80.03	19.97	80.01	9.97	-0.02
	89.97	10.03	90.03	9.97	+0.06

* %difference is the difference between the *m*-CNB composition in the feed with and without adsorbent.

From the table, it can be seen that the feed composition of *m*- and *p*-CNB before and after adding 5 grains of the KY zeolite in each composition are almost the same. These results are similar to Pattanapaiboonkul (2009) and Yairit (2010), who studied the effects of FAU zeolites and number of zeolite on the CNB feed solution compositions (61.0, 62.9, 65.0 wt% *m*-CNB) with NaX, CaX, BaX, NaY, CaY zeolite. In 2011, Neaungjumnong studied effect of FAU zeolites on the CNB feed solution compositions (62.9, 63.5 wt% *m*-CNB) with NaX, CaX, BaX, NaY, CaY, KY zeolite, SiO_2, Al_2O_3, activated carbon, and glass bead. The result shows that the feed compositions before and after adding the zeolite are similar. This implies that the presence of a zeolite hardly affects the *m*- and *p*-CNB compositions in the feed solution. In this case, the zeolite may not perform as an adsorbent. Instead, it may act like a foreign particle in the system, not an adsorbent.

4.2.2 Effects of KY Zeolite on the CNB Crystal Composition and Crystallization Temperature

The effects of KY zeolite on the CNB crystal composition and crystallization temperature were investigated. Five grains of the KY zeolite were added at the center of the CNB mixture in the crystallizer. Figure 4.3 shows locations, where crystals were collected for *m*- and *p*-CNB composition analysis. The crystallization temperature, feed and crystal composition are shown in Tables 4.5 and 4.6. The result shows that the crystal composition near the KY zeolite (area (a)) have the purity higher than those far from the zeolite (area (b)).With the presence of the KY zeolite, the crystallization of the feed with the composition below and above the eutectic composition results in the crystal form. Below the eutectic composition, the crystals are rich in *p*-CNB. At the eutectic composition, 62.9 wt% *m*-CNB, the feed can be crystallized at 20.0 °C. Unlike the system without the zeolite, where the amorphous solid is formed, the crystal formation is observed when the zeolite is present in the feed. The composition of the crystal is rich in *p*-CNB. The feed compositions at 70.0, 80.0, 90.0 wt% *m*-CNB (above the eutectic composition) result in the crystals rich in *m*-CNB. Interestingly, the crystallization of the feed above the eutectic composition, 65.0 wt% *m*-CNB, the crystal composition is shifted from being rich in *m*-CNB to rich in *p*-CNB.

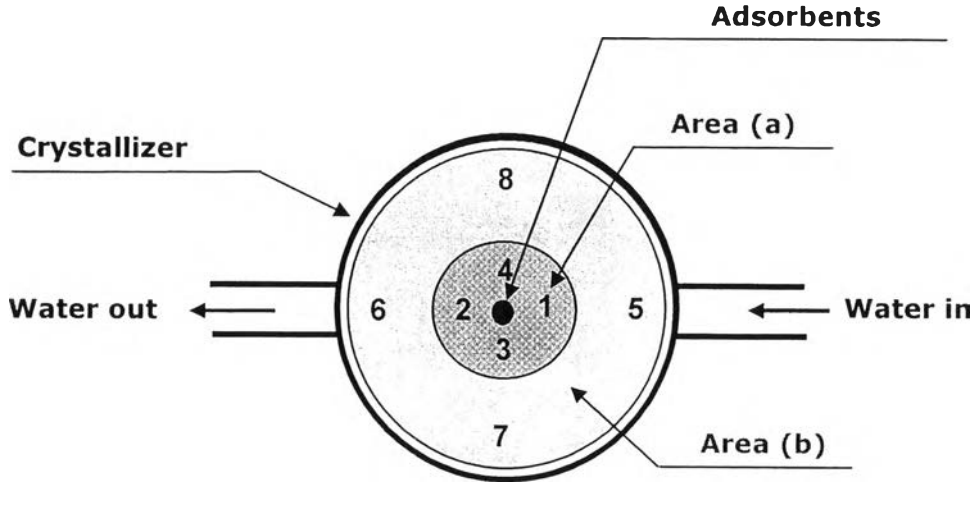

Figure 4.3 Locations where crystals were collected for *m*- and *p*-CNB composition analysis.

Table 4.5 Composition of *m*- and *p*-CNB in the crystals located near and far from adsorbents with 5 grains of KY zeolite Run#1

Feed composition (wt%)	Crystal near adsorbent			Crystal far from adsorbent			Crystallization temperature (°C)
	Composition (wt%)			Composition (wt%)			
	m-CNB	*p*-CNB	*m*-/*p*-CNB	*m*-CNB	*p*-CNB	*m*-/*p*-CNB	
20.01	2.86 **[1]**	97.14 **[1]**	0.0294	4.28 **[5]**	95.72 **[5]**	0.0447	67.0
	2.01 **[2]**	97.99 **[2]**	0.0205	4.71 **[6]**	95.29 **[6]**	0.0494	
	1.22 **[3]**	98.78 **[3]**	0.0124	4.18 **[7]**	95.82 **[7]**	0.0436	
	2.42 **[4]**	97.58 **[4]**	0.0248	3.68 **[8]**	96.32 **[8]**	0.0382	
30.03	1.60 **[1]**	98.40 **[1]**	0.0163	5.85 **[5]**	94.15 **[5]**	0.0621	57.0
	2.41 **[2]**	97.59 **[2]**	0.0247	3.00 **[6]**	97.00 **[6]**	0.0309	
	1.97 **[3]**	98.03 **[3]**	0.0201	4.84 **[7]**	95.16 **[7]**	0.0509	
	1.82 **[4]**	98.18 **[4]**	0.0185	1.82 **[8]**	98.18 **[8]**	0.0185	
40.02	2.73 **[1]**	97.27 **[1]**	0.0281	5.53 **[5]**	94.47 **[5]**	0.0585	48.0
	4.42 **[2]**	95.58 **[2]**	0.0462	4.64 **[6]**	95.36 **[6]**	0.0487	
	6.60 **[3]**	93.40 **[3]**	0.0707	6.12 **[7]**	93.88 **[7]**	0.0652	
	3.21 **[4]**	96.79 **[4]**	0.0332	5.46 **[8]**	94.54 **[8]**	0.0578	

* The number in the parenthesis refers to the position where crystals were collected as shown in Figure 4.3.

Table 4.5 (Cont.) Composition of *m*- and *p*-CNB in the crystals located near and far from adsorbents with 5 grains of KY zeolite Run#1

Feed composition (wt%)	Crystal near adsorbent			Crystal far from adsorbent			Crystallization temperature (°C)
	Composition (wt%)			Composition (wt%)			
	m-CNB	*p*-CNB	*m*-/*p*-CNB	*m*-CNB	*p*-CNB	*m*-/*p*-CNB	
61.03	7.27 **[1]**	92.73 **[1]**	0.0784	9.10 **[5]**	90.90 **[5]**	0.1001	23.0
	6.95 **[2]**	93.05 **[2]**	0.0747	8.98 **[6]**	91.02 **[6]**	0.0986	
	7.74 **[3]**	92.26 **[3]**	0.0839	10.25 **[7]**	89.75 **[7]**	0.1142	
	6.31 **[4]**	93.69 **[4]**	0.0673	9.56 **[8]**	90.44 **[8]**	0.1057	
62.93	8.06 **[1]**	91.94 **[1]**	0.0877	10.88 **[5]**	89.12 **[5]**	0.1221	20.0
	7.83 **[2]**	92.17 **[2]**	0.0849	10.92 **[6]**	89.08 **[6]**	0.1226	
	7.70 **[3]**	92.30 **[3]**	0.0834	10.78 **[7]**	89.22 **[7]**	0.1208	
	8.10 **[4]**	91.90 **[4]**	0.0881	11.25 **[8]**	88.75 **[8]**	0.1268	
65.02	11.19 **[1]**	88.81 **[1]**	0.1259	25.63 **[5]**	74.37 **[5]**	0.3446	23.5
	11.36 **[2]**	88.64 **[2]**	0.1282	22.08 **[6]**	77.92 **[6]**	0.2834	
	10.97 **[3]**	89.03 **[3]**	0.1232	23.51 **[7]**	76.49 **[7]**	0.3074	
	11.84 **[4]**	88.16 **[4]**	0.1343	24.60 **[8]**	75.40 **[8]**	0.3263	

* The number in the parenthesis refers to the position where crystals were collected as shown in Figure 4.3.

Table 4.5 (Cont.) Composition of *m*- and *p*-CNB in the crystals located near and far from adsorbents with 5 grains of KY zeolite Run#1

Feed composition (wt%)	Crystal near adsorbent			Crystal far from adsorbent			Crystallization temperature (°C)
	Composition (wt%)			Composition (wt%)			
	m-CNB	*p*-CNB	*m*-/*p*-CNB	*m*-CNB	*p*-CNB	*m*-/*p*-CNB	
70.00	93.61 **[1]**	6.39 **[1]**	14.6494	94.68 **[5]**	5.32 **[5]**	17.7969	25.0
	96.52 **[2]**	3.48 **[2]**	27.7356	92.41 **[6]**	7.59 **[6]**	12.7152	
	92.08 **[3]**	7.92 **[3]**	11.6263	92.58 **[7]**	7.42 **[7]**	12.4771	
	93.52 **[4]**	6.48 **[4]**	14.4321	94.00 **[8]**	6.00 **[8]**	15.6667	
80.04	98.60 **[1]**	1.40 **[1]**	70.4286	97.73 **[5]**	2.27 **[5]**	43.0528	28.5
	98.33 **[2]**	1.67 **[2]**	58.8802	95.69 **[6]**	4.31 **[6]**	22.2019	
	98.89 **[3]**	1.11 **[3]**	89.0900	98.68 **[7]**	1.32 **[7]**	74.7576	
	98.59 **[4]**	1.41 **[4]**	69.9219	96.83 **[8]**	3.17 **[8]**	30.5457	
90.01	98.22 **[1]**	1.78 **[1]**	55.1798	98.32 **[5]**	1.68 **[5]**	58.5238	33.0
	98.36 **[2]**	1.64 **[2]**	59.9756	97.36 **[6]**	2.64 **[6]**	36.8788	
	97.92 **[3]**	2.08 **[3]**	47.0769	97.88 **[7]**	2.12 **[7]**	46.1698	
	98.54 **[4]**	1.46 **[4]**	67.4932	97.77 **[8]**	2.23 **[8]**	43.8430	

* The number in the parenthesis refers to the position where crystals were collected as shown in Figure 4.3.

Table 4.6 Composition of *m*- and *p*-CNB in the crystals located near and far from adsorbents with 5 grains of KY zeolite Run#2

Feed composition (wt%)	Crystal near adsorbent			Crystal far from adsorbent			Crystallization temperature (°C)
	Composition (wt%)			Composition (wt%)			
	m-CNB	*p*-CNB	*m*-/*p*-CNB	*m*-CNB	*p*-CNB	*m*-/*p*-CNB	
20.04	3.12 **[1]**	96.88 **[1]**	0.0322	5.68 **[5]**	94.32 **[5]**	0.0602	68.0
	2.46 **[2]**	97.54 **[2]**	0.0252	3.09 **[6]**	96.91 **[6]**	0.0319	
	2.27 **[3]**	97.73 **[3]**	0.0232	2.18 **[7]**	97.82 **[7]**	0.0223	
	1.86 **[4]**	98.14 **[4]**	0.0189	2.77 **[8]**	97.23 **[8]**	0.0285	
29.97	2.32 **[1]**	97.68 **[1]**	0.0238	2.90 **[5]**	97.10 **[5]**	0.0299	57.0
	1.49 **[2]**	98.51 **[2]**	0.0151	2.78 **[6]**	97.22 **[6]**	0.0286	
	2.51 **[3]**	97.49 **[3]**	0.0257	5.13 **[7]**	94.87 **[7]**	0.0541	
	3.16 **[4]**	96.84 **[4]**	0.0326	3.47 **[8]**	96.53 **[8]**	0.0359	
40.01	2.62 **[1]**	97.38 **[1]**	0.0269	6.07 **[5]**	93.93 **[5]**	0.0646	48.0
	5.78 **[2]**	94.22 **[2]**	0.0613	3.87 **[6]**	96.13 **[6]**	0.0403	
	3.34 **[3]**	96.66 **[3]**	0.0346	4.46 **[7]**	95.54 **[7]**	0.0467	
	2.92 **[4]**	97.08 **[4]**	0.0301	3.91 **[8]**	96.09 **[8]**	0.0407	

* The number in the parenthesis refers to the position where crystals were collected as shown in Figure 4.3.

Table 4.6 (Cont.) Composition of *m*- and *p*-CNB in the crystals located near and far from adsorbents with 5 grains of KY zeolite Run#2

Feed composition (wt%)	Crystal near adsorbent			Crystal far from adsorbent			Crystallization temperature (°C)
	Composition (wt%)			Composition (wt%)			
	m-CNB	*p*-CNB	*m*-/*p*-CNB	*m*-CNB	*p*-CNB	*m*-/*p*-CNB	
61.06	6.26 **[1]**	93.74 **[1]**	0.0668	7.60 **[5]**	92.40 **[5]**	0.0822	23.0
	5.39 **[2]**	94.61 **[2]**	0.0569	9.74 **[6]**	90.26 **[6]**	0.1079	
	5.17 **[3]**	94.83 **[3]**	0.0545	8.03 **[7]**	91.97 **[7]**	0.0873	
	6.49 **[4]**	93.51 **[4]**	0.0694	11.97 **[8]**	88.03 **[8]**	0.1359	
62.95	8.68 **[1]**	91.32 **[1]**	0.0951	10.13 **[5]**	89.87 **[5]**	0.1127	20.0
	9.83 **[2]**	90.17 **[2]**	0.1090	12.20 **[6]**	87.80 **[6]**	0.1389	
	7.13 **[3]**	92.87 **[3]**	0.0768	11.10 **[7]**	88.90 **[7]**	0.1249	
	6.80 **[4]**	93.20 **[4]**	0.0729	11.30 **[8]**	88.70 **[8]**	0.1274	
65.03	11.39 **[1]**	88.61 **[1]**	0.1285	15.23 **[5]**	84.77 **[5]**	0.1797	23.5
	9.13 **[2]**	90.87 **[2]**	0.1005	12.20 **[6]**	87.80 **[6]**	0.1389	
	5.97 **[3]**	94.03 **[3]**	0.0635	18.92 **[7]**	81.08 **[7]**	0.2333	
	9.79 **[4]**	90.21 **[4]**	0.1085	21.36 **[8]**	78.64 **[8]**	0.2716	

* The number in the parenthesis refers to the position where crystals were collected as shown in Figure 4.3.

Table 4.6 (Cont.) Composition of *m*- and *p*-CNB in the crystals located near and far from adsorbents with 5 grains of KY zeolite Run#2

Feed composition (wt%)	Crystal near adsorbent			Crystal far from adsorbent			Crystallization temperature (°C)
	Composition (wt%)			Composition (wt%)			
	m-CNB	*p*-CNB	*m*-/*p*-CNB	*m*-CNB	*p*-CNB	*m*-/*p*-CNB	
69.96	95.36 **[1]**	4.64 **[1]**	20.5517	93.22 **[5]**	6.78 **[5]**	13.7493	25.0
	97.11 **[2]**	2.89 **[2]**	33.6021	91.37 **[6]**	8.63 **[6]**	10.5875	
	94.55 **[3]**	5.45 **[3]**	17.3486	90.20 **[7]**	9.80 **[7]**	9.2041	
	92.90 **[4]**	7.10 **[4]**	13.0845	91.90 **[8]**	8.10 **[8]**	11.3457	
80.03	97.07 **[1]**	2.93 **[1]**	33.1297	97.82 **[5]**	2.18 **[5]**	44.8716	28.5
	97.89 **[2]**	2.11 **[2]**	46.3934	94.38 **[6]**	5.62 **[6]**	16.7936	
	98.54 **[3]**	1.46 **[3]**	67.4932	95.71 **[7]**	4.29 **[7]**	22.3100	
	98.24 **[4]**	1.76 **[4]**	55.8182	98.03 **[8]**	1.97 **[8]**	49.7614	
89.97	98.59 **[1]**	1.41 **[1]**	69.9219	96.58 **[5]**	3.42 **[5]**	28.2398	33.0
	98.30 **[2]**	1.70 **[2]**	57.8235	97.12 **[6]**	2.88 **[6]**	33.7222	
	98.19 **[3]**	1.81 **[3]**	54.2486	97.48 **[7]**	2.52 **[7]**	38.6825	
	96.41 **[4]**	3.59 **[4]**	26.8552	95.74 **[8]**	4.26 **[8]**	22.4742	

* The number in the parenthesis refers to the position where crystals were collected as shown in Figure 4.3.

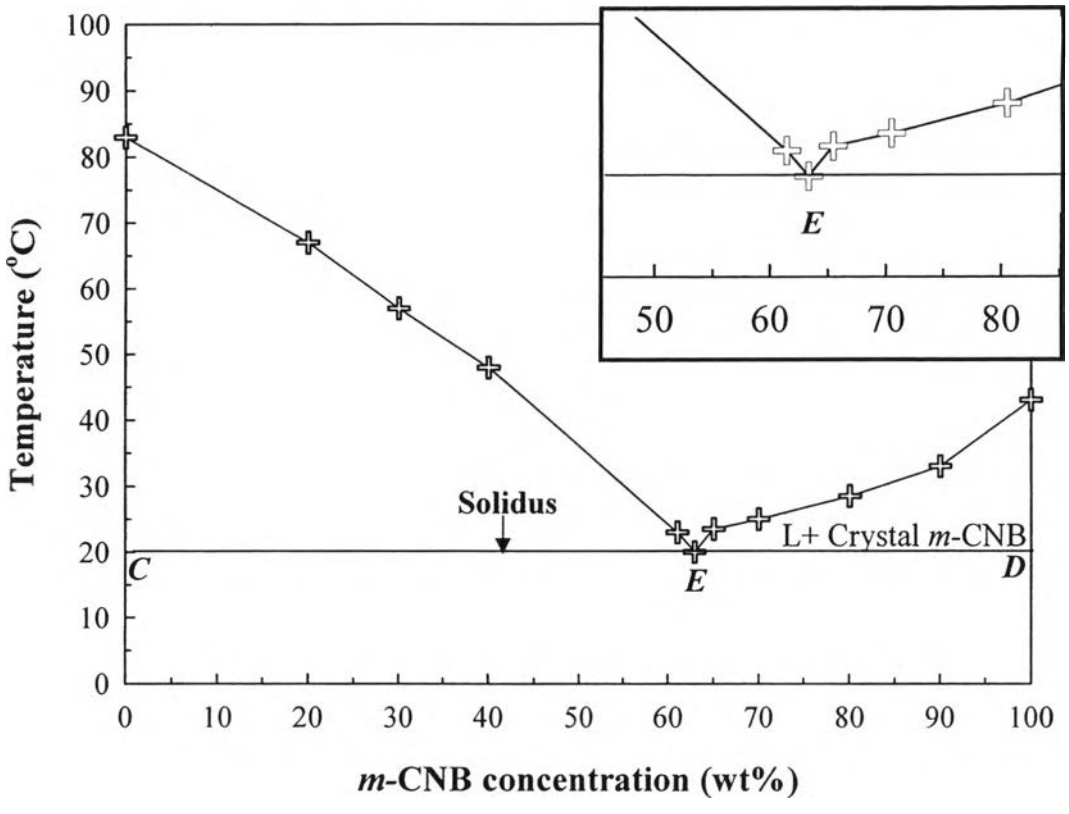

Figure 4.4 Binary phase diagram of *m*- and *p*-CNB with the presence of the KY zeolite.

The binary phase diagram of *m*- and *p*-CNB with the presence of the KY zeolite is shown in Figure 4.4. Above the ***AEB*** curve (the liquidus) is homogeneous liquid *m*-CNB and *p*-CNB. Below the ***CED*** line (the solidus) is solid. Below the eutectic composition (20.0, 30.0, 40.0 and 61.0 wt% *m*-CNB), where the feed solution is cooled down to the crystallization temperature, the crystal solid of *p*-CNB forms. When the feed solutions above the eutectic composition (65.0, 70.0, 80.0 and 90.0 wt% *m*-CNB) is cooled down, the *m*-CNB solid crystal form is obtained. The sectors ***ACE*** and ***BDE*** contain mixtures of crystal *p*-CNB + solution of *m*- and *p*-CNB and crystal *m*-CNB + solution of *m*- and *p*-CNB, respectively. Point ***E*** represents the temperature and composition of the eutectic. The eutectic composition in this phase diagram is 62.9 wt% *m*-CNB and 37.1 wt% *p*-CNB with the crystallization temperature is 20.0 °C. Unlike the system without the zeolite, the crystal formation is observed when the zeolite is present in the feed. The composition of the crystal is rich in *p*-CNB. Interestingly, with the feed composition of 65.0 wt%

m-CNB (above the eutectic composition), the crystal composition is shifted from being rich in *m*-CNB to rich in *p*-CNB.

The binary phase diagram of *m*- and *p*-CNB with and without the KY zeolite is shown in Figure 4.5. It can be seen that the binary phase diagram of *m*- and *p*-CNB with the presence of the KY zeolite is similar to that without the zeolite. The crystallization temperature at the eutectic composition of the system with the zeolite is shifted from 23.0 °C to 20.0 °C. With the presence of the zeolite in the CNB mixture, the crystallization temperature is lower than that in the system without the zeolite.

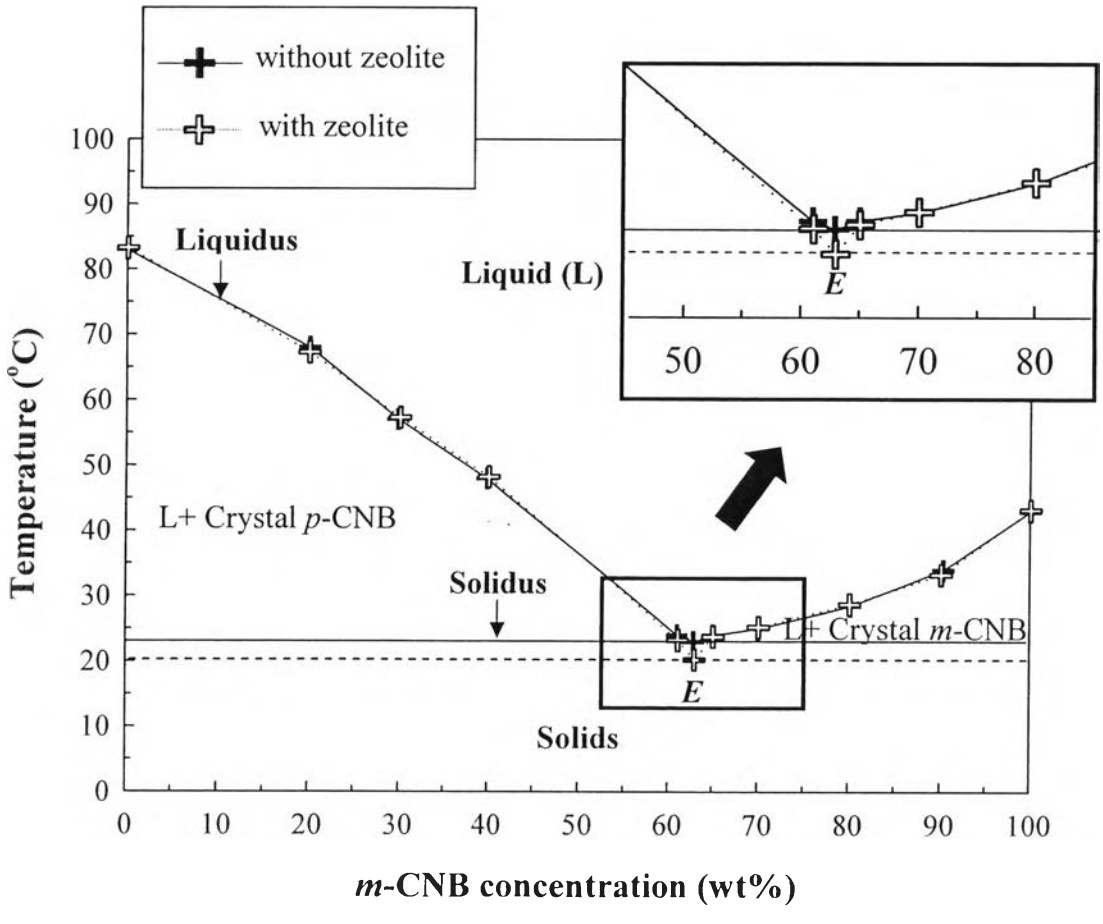

Figure 4.5 Binary phase diagram of *m*- and *p*-CNB with and without the KY zeolite.

Two interesting phenomena can be observed in this study: 1) The amorphous solid form is changed to the crystal form, when the feed with the eutectic composition is crystallized, and 2) The crystal composition is shifted being rich in *m*-

CNB to *p*-CNB with the feed with 65 wt% CNB is crystallized. A possible reason may be related to the presence of foreign particles in the feed solution. The presence of foreign particle or impurity in the system can affect the nucleation step. It can induce primary nucleation in the heterogeneous nucleation. The feed solution can form on those nuclei surfaces with lower supersaturation as shown in Figure 4.6. However, the influence of agitation on the nucleation step is very complex. No general rule applies, and each case should be considered separately (Mullin, 2001). Another reason may come from the metastable zone width and interfacial tension. In the crystallization processes, supersaturated solutions exhibit a metastable zone. The metastable zone width results from the specific characteristics of nucleation in a supersaturated solution of soluble substances. The metastable zone width is considered as a characteristic property of crystallization, and depends on temperature, solution, cooling rate, and presence of impurity.

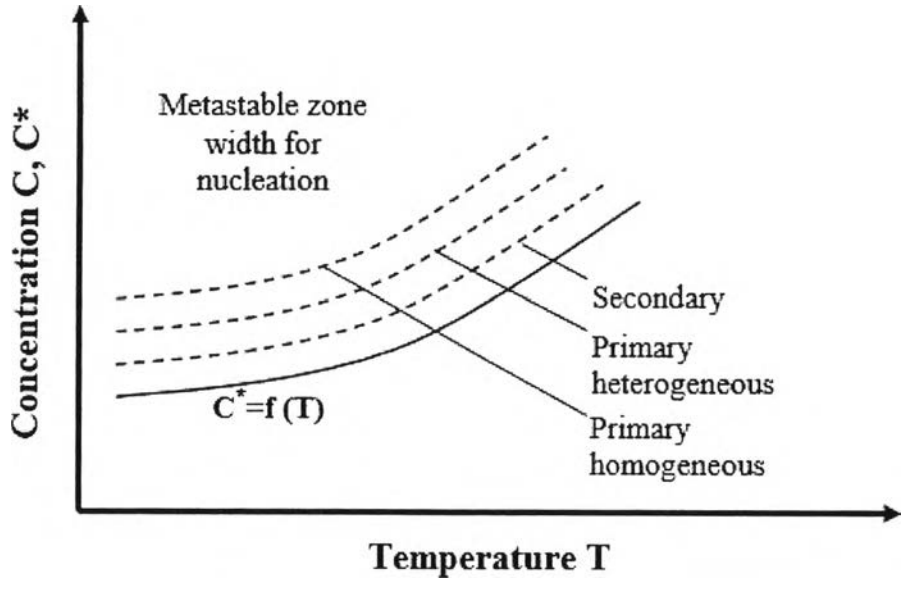

Figure 4.6 Concentration against temperature for several types of nucleation Processes (sundoc.bibliothek.uni-halle.de).

The relationship between supersaturation and spontaneous crystallization led to a diagrammatic representation of the metastable zone on a solubility-supersolubility diagram, as shown in Figure 4.7. The lower continuous solubility curve can be located with precision. The upper broken supersolubility curve, which represents temperatures and concentrations, at which uncontrolled spontaneous crystallization occurs, is not as well defined as that of the solubility curve. Its position in the diagram is considerably affected by, amongst other things, the rate, at which supersaturation is generated, the intensity of agitation, the presence of trace impurities, and the thermal history of the solution. The diagram is divided into three zone (Mullin, 2001):

1. The stable (unsaturated) zone, where crystallization is impossible.
2. The metastable (supersaturated) zone, between the solubility and supersolubility curve, where spontaneous crystallization is impossible. However, if a crystal seed is placed in such a metastable solution, growth could occur on it.
3. The unstable or labile (supersaturated) zone, where spontaneous crystallization is possible, but not inevitable.

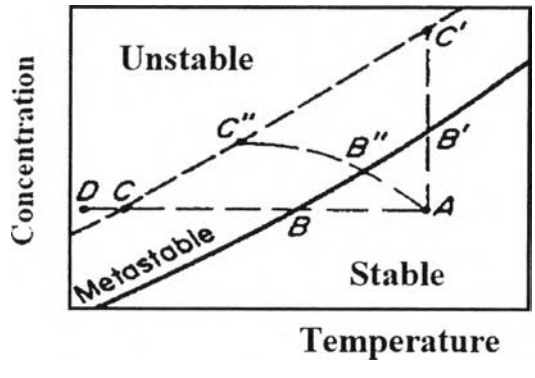

Figure 4.7 Solubility-supersolubility diagram (Mullin, 2001).

If a solution represented by point *A* in Figure 4.7 is cooled without loss of solvent (line *ABC*), spontaneous crystallization cannot occur until conditions represented by point *C* are reached. At this point, crystallization may be spontaneous or it may be induced by seeding, agitation or mechanical shock. Further cooling to

some point *D* may be necessary before crystallization can be induced (Mullin, 2001). The position in the diagram is considerably effected by the presence of trace impurities so that the presence of the KY zeolite in the CNB mixture may change the position in the diagram as well.

The maximum allowable supersaturation, Δc_{max}, may be expressed in terms of the maximum allowable undercooling, $\Delta\theta_{max}$:

$$\Delta c_{max} = \left(\frac{dc^*}{d\theta}\right)\Delta\theta_{max} \tag{4.4}$$

As the presence of a suitable foreign body or 'sympathic' surface can induce nucleation at degree of supercooling lower than those required for spontaneous nucleation (Mullin, 2001). This sentence is consistent with crystallization temperature in the presence of adsorbent, which is lower than in the absence of adsorbent. When the degree of supercooling decreases, $\Delta\theta_{max}$ and Δc_{max} increase according to the relationship between $\Delta\theta_{max}$ and Δc_{max} in Equation (4.4). Increasing $\Delta\theta_{max}$ and Δc_{max} results in a broader metastable zone width.

The overall free energy change associated with the formation of a critical nucleus under heterogeneous conditions, ΔG_{het}, must be less than the corresponding free energy change, ΔG_{homo}, associated with homogeneous nucleation, i.e. (Mullin, 2001).

$$\Delta G_{het} = \phi\,\Delta G_{homo} \tag{4.5}$$

where the factor ϕ is less than unity.

The interfacial tension, γ, is one of the important factors controlling the nucleation process. Figure 4.8 shows a contact angle and interfacial energy diagram. The three interfacial tensions are denoted by γ_{cl}, γ_{sl}, and γ_{cs}. Resolving these forces in a horizontal direction

$$\gamma_{sl} = \gamma_{cs} + \gamma_{cl} \cos\theta \tag{4.6}$$

or the contact angle θ is determined by Young's relation

$$\cos\theta = \frac{\gamma_{sl} - \gamma_{cs}}{\gamma_{cl}} \tag{4.7}$$

The angle, θ, of contact between the crystalline deposit and foreign solid surface, corresponds to the angle of wetting in liquid-solid system (Mullin, 2001).

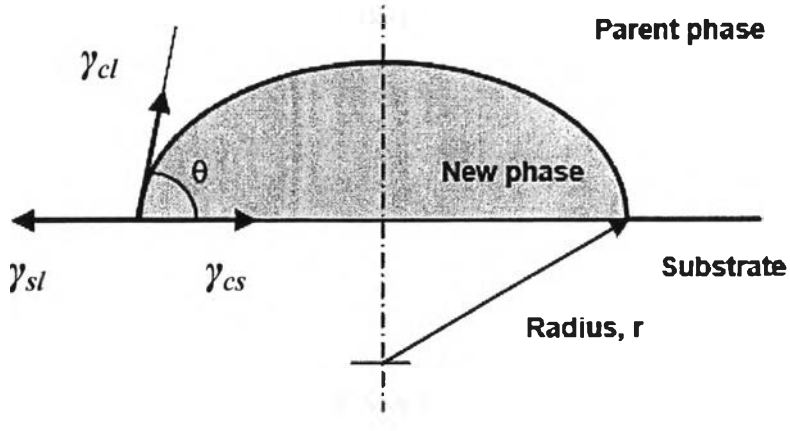

Figure 4.8 Contact angle and interfacial tension (sundoc.bibliothek.uni-halle.de).

The factor ϕ in Equation 4.5 can be express as

$$\phi = \frac{(2 + \cos\theta)(1 - \cos\theta)^2}{4} \tag{4.8}$$

Thus, when $\theta = 180°$, $\cos\theta = -1$ and $\phi = 1$, Equation 4.5 becomes

$$\Delta G_{het} = \Delta G_{homo} \tag{4.9}$$

When θ lines between 0 and 180°, $\phi < 1$; therefore,

$$\Delta G_{het} < \Delta G_{homo} \tag{4.10}$$

When $\theta = 0$, $\phi = 0$, and

$$\Delta G_{het} = 0 \tag{4.11}$$

The wetting angle determines the ease of nucleation by reducing the energy needed. The barrier energy needed for heterogeneous nucleation is reduced.

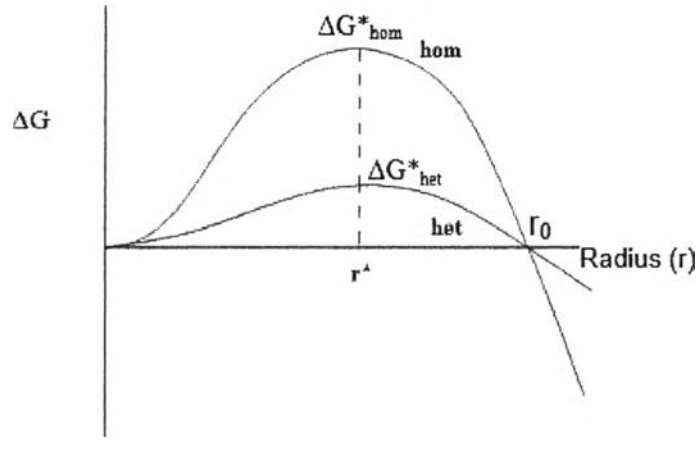

Figure 4.9 Barrier energy needed for heterogeneous nucleation (eng.utah.edu).

This is illustrated in Figure 4.10, which shows a foreign particle in a supersaturated solution (Mersmann, 2001).

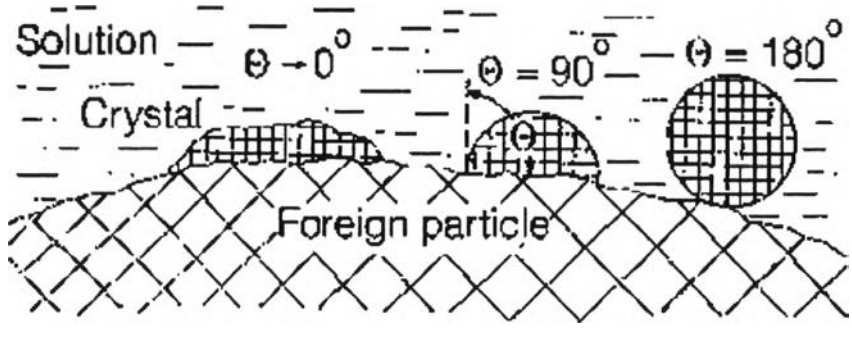

Figure 4.10 Nucleation on a foreign particle for different wetting angles (Mersmann, 2001).

For the case of complete non-affinity between the crystalline solid and the foreign solid surface (corresponding to that of complete non-wetting in liquid-solid system), θ=180°, and Equation (4.9) applies, i.e. the overall free energy of nucleation is the same as that required for homogeneous or spontaneous nucleation. For the case partial affinity (cf. the partial wetting of a solid with a liquid), $0<\theta<180°$, and Equation (4.10) applies, which indicates that nucleation is easier to achieve because the overall excess free energy required is less than that for homogeneous nucleation. For the case of complete affinity (cf. complete wetting) θ=0, and the free energy of nucleation of zero. This case corresponds to the seeding of a supersaturation solution with crystals of the required crystalline product, i.e. no nuclei have to be formed in the solution (Mullin, 2001).

The presence of an adsorbent may be in the case of the partial wetting of a solid with a liquid, which is described by Equation (4.10), and ΔG_{homo} is related to $(\Delta T)^{-2}$ as indicated in Equation (4.12).

$$\Delta G_{homo} \propto (\Delta T)^{-2} \tag{4.12}$$

where $\Delta T = T^* - T$ is the supercooling, T^* is the solid-liquid equilibrium temperature, and T is degree of supersaturation (Mullin, 2001).

From Equation (4.5), (4.10) and (4.12), the value of ΔG_{het} will be less than ΔG_{homo} when the value of ΔT is high that means the value of T or degree of supersaturation must be low. This relates to "The presence of a suitable foreign body or 'sympathic' surface can induce nucleation at degree of supercooling lower than those require for spontaneous nucleation (Mullin, 2001)." The metastable zone width may become broader. Thus, the crystallization temperature of the feed solution with the KY zeolite decreases from the crystallization temperature of the feed solution without any adsorbent (Mullin, 2001).